An aqueous cathodic delamination route towards high quality graphene flakes for oil sorption and electrochemical charge storage applications

Sergio García-Dalí, Juan I. Paredes,* José M. Munuera, Silvia Villar-Rodil,* Amelia Martínez-Alonso, Juan M.D. Tascón

Instituto Nacional del Carbón, INCAR-CSIC, C/Francisco Pintado Fe 26, 33011 Oviedo, Spain

* Corresponding author: paredes@incar.csic.es

* Corresponding author: silvia@incar.csic.es

Abstract

The electrochemical exfoliation of graphite in aqueous medium stands out as an attractive, scalable approach for the production of graphenes for different applications, due to its simplicity, cost-effectiveness and environmental friendliness. In particular, cathodic exfoliation in water should allow access to high quality, non-oxidized graphene flakes, as it avoids the intrinsic oxidizing conditions that typically plague the anodic route, but this possibility has been limited by a poor intercalation ability of aqueous cations. Here, we demonstrate that with a proper choice of starting graphite and electrolyte, high quality graphene flakes can be obtained in substantial yields via cathodic delamination in water. Graphites having some pre-expanded edges and interlayer voids (e.g., graphite foil) were found to be critical for a successful exfoliation. Large differences in the efficiency of a range of aqueous quaternary ammonium-based electrolytes were observed, quantitatively compared and rationalized on the basis of their chemical structure. Graphene yields up to 40–50 wt% were attained with the most efficient cations (tetrapropylammonium and hexyltrimethylammonium). Hydrophobic sponges made up of cathodic graphene-coated melamine foam exhibited a notable capacity towards the sorption of oils and organic solvents from water with good re-usability. Hybrids comprised of cathodically exfoliated graphite and a small amount of vertically oriented cobalt oxide nanosheets displayed good electrochemical charge storage behavior. Overall, the ability to access graphene flakes in considerable yields by the aqueous cathodic route disclosed here should raise the prospects of cathodic exfoliation as a competitive method for the industrial manufacturing of high quality graphene for practical applications.

Keywords: two-dimensional (2D) material, graphene, cobalt oxide, electrochemical exfoliation, water remediation, energy storage.

1. Introduction

Current efforts on the research field of graphene are mostly focused on translating its attractive features to a plethora of relevant technological applications. Indeed, its high surface area and electrical conductivity, make it a promising candidate for applications in the fields of energy conversion and storage [1–3] and water remediation [4,5], among others. However, for a successful performance in those applications, the individual accessible area of each graphene nanosheet has to be preserved. Typical strategies have involved assembling the two-dimensional (2D) graphene nanosheets into three-dimensional structures through complex, time-consuming and costly processes [6,7]. An interesting alternative to such strategies could be the production of graphene by electrochemical exfoliation of graphite [8–13], which directly provides three-dimensional networks of loosely connected graphene sheets [14] by a simple, quick, cost-effective and scalable process. This top-down approach relies on the delamination of a graphite electrode triggered by intercalation of ions from an electrolytic medium upon application of a DC bias voltage. By its own nature, the electrochemical exfoliation method can be implemented under two distinct operation modes, namely, the anodic mode and the cathodic mode. The former is typically carried out in aqueous electrolytes of common inorganic acids (e.g., H_2SO_4) or their salts [$(NH_4)_2SO_4$, Na_2SO_4, etc], and generally affords well exfoliated graphene nanosheets (< 5 monolayers thick) in high yields [10,11]. Nonetheless, these electrolytes tend to give anodically exfoliated graphene that is substantially oxidized due to attack by highly reactive oxygen radicals (e.g., ·OH) generated from the anodic oxidation of water molecules, thus compromising

its utility in applications that demand high quality materials. Although recent work has demonstrated that such an oxidative attack can be avoided to a considerable degree, it normally requires resorting to more complex and expensive electrolytes and/or electrolyte additives, which act as oxygen radical scavengers [15–17], but this strategy can also risk a lower efficiency of the intercalation/exfoliation process itself [14,16].

On the other hand, extensive oxidation of graphene is inherently averted in cathodic exfoliation due to the fact that the graphite electrode is subjected to reducing conditions (negative potential). This delamination mode has been demonstrated to yield high quality, largely defect-free graphenes using electrolytic media that are typically based on lithium [18,19], sodium [20], alkylammonium [21–23], alkylimidazolium [24,25] or alkylpyrrolidinium [24,26,27] salts in such organic solvents as propylene carbonate, acetonitrile, dimethyl sulfoxide or *N*,*N*-dimethylformamide. However, carrying out cathodic exfoliation in aqueous (rather than organic) electrolytic media would be highly desirable, as it would make the production process easier to scale-up as well as more environmentally friendly and affordable, but, with the exception of a very recent work [28], this possibility has been seldom reported [29]. A likely reason behind this state of affairs is that because the graphite electrode does not oxidize under the applied cathodic potential, its hydrophobic interlayer spaces cannot be efficiently intercalated by the hydrated cations from the electrolyte (as opposed to the case of the hydrated anions in anodic exfoliation). As a result, only "naked", de-hydrated cations will be probably able to intercalate the graphite cathode, and if they cannot enter in sufficient numbers and/or they do not have the right molecular size, the graphite layers will not be pushed apart from each other to an extent enough to allow exfoliation.

When cathodic exfoliation is accomplished in organic solvents, the efficiency of graphite delamination is known to depend not only on the specific type of intercalating

cation used, but also on the organic solvent itself, i.e., the success of exfoliation is determined by the choice of a proper cation/organic solvent combination [30,31]. We hypothesized that a similar situation could be in place for aqueous electrolytes, implying that, among other possible factors, the selection of the intercalating cation should be crucial for an effective exfoliation in water. Indeed, there is some evidence in the recent literature suggesting that this hypothesis is correct [32]. More specifically, aqueous tetrabutylammonium cations were shown to increase the delamination yield of graphite electrodes in conjunction with sulfate anions in a combined anodic/cathodic process, whereas such an effect was much weaker or even not present at all with other tested cations (i.e., tetramethylammonium and ammonium). However, to the best of our knowledge a thorough survey aimed at identifying the most efficient cations in purely cathodic exfoliation processes has not yet been undertaken.

We have investigated a broad range of ammonium-based cations as prospective intercalating/exfoliating agents for the cathodic delamination of graphite into graphene in aqueous medium, the results of which are reported here. Very large differences in the ability of these chemical species to intercalate and expand the graphite electrode were observed, quantitatively compared and rationalized on the basis of their chemical make-up. More significantly, the tested cations that turned out to be the most efficient in terms of their expanding power were shown to afford graphene nanosheets in competitive yields, which should facilitate the future industrial implementation of the cathodic route as a method of choice for the manufacturing of high quality graphenes. We demonstrate the potential of this type of graphene nanosheets in practical applications with two specific examples, namely, (1) the sorption of oils and organic solvents either using the as-prepared, stand-alone graphene material directly obtained from the cathodic process or using melamine foam coated with the cathodically exfoliated nanosheets, and (2) the

use of the cathodic graphene in combination with cobalt oxide nanosheets as an electrode for electrochemical charge storage.

2. Materials and methods

2.1. Materials and reagents

Three types of high-purity graphite were used in the electrochemical exfoliation experiments, namely, graphite foil, graphite rod and highly oriented pyrolytic graphite (HOPG). Graphite foil (Papyex I980) with a thickness and mass density of ~500 μm and 1.1 g cm^{-3}, respectively, was acquired from Mersen. Graphite rod (diameter: 3.05 mm; density: 1.7 g cm^{-3}) was purchased from Alfa Aesar, whereas HOPG (grade ZYH, density: 2.25 g cm^{-3}) was obtained from Advanced Ceramics. Unless stated otherwise, all the chemicals used throughout the study (salts, organic solvents, reagents, etc) were received from Sigma-Aldrich. The following salts were used for the preparation of the aqueous electrolytic media for cathodic exfoliation: ammonium chloride (ACl), trimethylamine hydrochloride (TMAHCl), tetramethylammonium chloride (TMACl), tetraethylammonium chloride (TEACl), tetrapropylammonium chloride (TPACl), tributylamine hydrochloride (TBAHCl), tributylmethylammonium chloride (TBMACl), tetrabutylammonium chloride (TBACl), hexyltrimethylammonium bromide (HTMABr), octyltrimethylammonium bromide (OTMABr), dodecyltrimethylammonium bromide (DDTMABr), hexadecyltrimethylammonium bromide (HDTMABr), phenyltrimethylammonium chloride (PhTMACl) and benzyltrimethylammonium chloride (BzTMACl). Critical micelle concentration (cmc) in mM for some of the previous salts which, being soluble amphiphiles, can undergo micellization and act as cationic surfactants are: ~0.993 (HTMABr), ~264 (OTMABr), 16 (DDTMABr), 0.9 (HDTMABr) [33,34]. Organic solvents for colloidal dispersion of the cathodic graphene

nanosheets: *N*-methyl-2-pyrrolidone (NMP), N-ethyl-2-pyrrolidone (NEP), N-vinyl-2-pyrrolidone (NVP), *N*,*N*-dimethylformamide (DMF), dimethyl sulfoxide (DMSO), 1,3-dioxolane and pyridine. Organic liquids for sorption tests: toluene, heptane, dodecane, tetrahydrofuran, acetone and chloroform. Oils for sorption tests: Commercial olive oil, commercial rotary vane pump. Commercial melamine foam (density ~8–10 mg cm^{-3}) was used as a scaffold for graphene in sorption tests. Other chemical reagents, surfactants and salts for synthesis: cobalt (II) acetate tetrahydrate, hexamethylenetetramine and Pluronic P123 (block copolymer surfactant). Milli-Q deionized water (resistivity: 18.2 MΩ·cm; Millipore Corporation) was used in all the experiments.

2.2. Cathodic exfoliation experiments

The cathodic exfoliation tests were undertaken in a two-electrode configuration, using a graphite piece as the cathode, platinum foil (dimensions: 25 × 25 × 0.025 mm^3) as the anode, and an aqueous solution of a given ammonium-based salt as the electrolytic medium. Most of the experiments were carried out with graphite foil (55 × 30 × 0.5 mm^3), although for comparative purposes HOPG (10 × 5 × 0.5 mm^3) and graphite rod (diameter: 3.05 mm; length: 40 mm) were also employed. The graphite cathode and platinum foil were immersed in the electrolytic solution (80 mL) at a distance of ~2 cm from each other and connected to the current source (Agilent 6614C DC power supply) through crocodile clips. A negative potential (typically -10 V) was subsequently applied to the graphite electrode for 2 h, during which the material was generally seen to swell and expand in different proportions depending on the specific salt used as an electrolyte, with some expanded graphite fragments of millimeter dimensions detaching from the cathode and being left to float on the aqueous solution.

After the electrolytic treatment, the fraction of the graphite foil that was expanded was gently scrapped from the cathode with a spatula and collected together with the detached graphite fragments. This product was then extensively washed with water (1.5 L) through filter paper to remove remnants of the ammonium-based salt, and finally allowed to dry at room temperature in air for one day and overnight under reduced pressure at 60 °C. To extract individual graphene nanosheets from the expanded product, the latter product was transferred to a certain organic solvent (NMP, NEP, NVP, DMF, DMSO, 1,3-dioxolane or pyridine) or to an aqueous solution of the surfactant Pluronic P123 (0.7 mg mL^{-1}) and sonicated for 3 h in an ultrasound bath cleaner (J.P. Selecta Ultrasons system, 40 kHz). The resulting suspension was left to stand undisturbed for 24 h or, alternatively, centrifuged at 100g for 20 min, after which the supernatant was collected and stored for further use, with the sediment being discarded. Following previously reported procedures [35] the concentration of graphene nanosheets in the supernatant dispersion was estimated by means of UV-vis absorption spectroscopy on the basis of the Lambert-Beer law, measuring the absorbance of the dispersion at a wavelength of 660 nm and using an extinction coefficient value of α_{660} = 2440 mL mg^{-1} m^{-1}.

2.3. Characterization techniques

The samples were characterized by UV-vis absorption spectroscopy, field-emission scanning electron microscopy (FE-SEM), scanning transmission electron microscopy (STEM), atomic force microscopy (AFM), Raman spectroscopy and X-ray photoelectron spectroscopy (XPS). UV-vis absorption spectra were obtained with a double-beam Hελios α spectrophotometer (Thermo Spectronic). FE-SEM and STEM images were recorded on a Quanta FEG 650 apparatus (FEI Company) working at a

voltage of 20–25 kV. Specimens for FE-SEM were directly mounted onto metallic sample holders using double-sided carbon adhesive tape, whereas for STEM the samples were first dispersed in a water/isopropanol mixture (50/50, v/v) by bath-sonication for 3 h (J.P. Selecta Ultrasons system, 40 kHz, power ~20 W L^{-1}) and then drop-cast (~150 μL) onto a copper grid (200 square mesh) covered with a thin, continuous carbon film (Electron Microscopy Sciences). AFM imaging was carried out in the tapping mode of operation with a Nanoscope IIIa Multimode microscope (Veeco), using silicon cantilevers with nominal spring constant and resonance frequency of ~40 N m^{-1} and 250–300 kHz, respectively. HOPG was employed as a supporting substrate for AFM, onto which an aqueous dispersion of the sample (prepared by bath-sonication) was deposited by drop-casting. Raman spectroscopy was conducted in a LabRam apparatus (Horiba Jobin Yvon) with a laser excitation wavelength of 532 nm. For XPS, a SPECS apparatus working at a pressure of 10^{-7} Pa and using a non-monochromatic Mg K_α X-ray source (11.81 kV, 100 W) was employed. Specimens for both Raman and XPS analysis were prepared by drop-casting graphene dispersions onto a metallic sample-holder pre-heated at ~50–60 ºC and allowing them to dry under ambient conditions until a uniform film was seen to cover the substrate. For the measurement of electrical conductivity, free-standing paper-like films were prepared by vacuum-filtration of graphene dispersions in NMP through a hydrophilic PTFE membrane filter (47 mm in diameter and 0.1 μm of pore size, from Merck Millipore). Then, 12 × 12 mm^2 square pieces were cut from the film and their conductivity determined by the van der Pauw method using a homemade setup (Agilent 6614C DC power source and Fluke 45 digital multimeter). The thickness of the films was estimated by FE-SEM and independently with a digital micrometer.

2.4. Testing of cathodically exfoliated graphene as a sorbent for oils/organic solvents and as an electrode for capacitive energy storage

The cathodic graphenes were tested as sorbents for organic solvents and oils, and as electrodes for electrochemical charge storage. Two types of graphene-based materials were tested as sorbents: (i) the as-expanded materials obtained with 0.3 M TPACl and 0.3 M HTMABr, i. e., the products directly obtained from the cathodic delamination process without a subsequent sonication step (only washed with water to remove remnants of the electrolyte), and (ii) cathodic graphene nanosheets extracted from the as-expanded product (0.3 M TPACl) through sonication and coated onto melamine foam. To prepare the graphene-coated melamine foam, a graphene dispersion at a concentration of ~0.25 mg mL^{-1} was first prepared by bath sonication of the as-expanded graphite in pyridine for 3 h. Then, a ~1 cm^3 cube of commercial melamine foam was soaked into the dispersion for 1 min and subsequently heated on a hot plate for 5 min to evaporate the solvent. The graphene loading was determined as the weight difference between the uncoated and the coated melamine foam cube. The soaking/evaporation process was repeated three or four times up to graphene loadings of 4 mg cm^{-3} onto the foam. For the sorption of oils and organic solvents, a certain mass of powdery, expanded material (typically 10–15 mg) was first put in a 1.5 mL vial. Then, small known volumes of a given oil/solvent (usually ~50 μL) were successively dropped on the material, which took them up until a point was reached where the sorbent became saturated and the liquid was seen to overflow the powder by the naked eye. Such a saturation point allowed estimating the total volume of oil/solvent retained by the sorbent. Similarly, the sorption capacity of the graphene-coated foams was calculated from the maximum volume of liquid that they were seen to absorb without dripping, which was transformed into the weight of adsorbed oil/solvent using the

following densities for each liquid: toluene (0.865 g cm^{-3}), *n*-hexane (0.63 g cm^{-3}), dodecane (0.75 g cm^{-3}), tetrahydrofuran (0.886 g cm^{-3}), acetone (0.79 g cm^{-3}), chloroform (1.492 g cm^{-3}), olive oil (0.91 g cm^{-3}) and pump oil (0.86 g cm^{-3}). The sorption capacities of both types of sorbent are given as the weight of solvent/oil retained per weight of sorbent, that is, per weight of as expanded material in the former case and per weight of graphene-coated foam in the latter. For the reusability tests, the foams were regenerated through extraction of the absorbed liquid by squeezing the foam between the handles of a pair of tweezers and gathering the desorbed liquid on absorbent paper.

The electrochemical energy storage experiments were carried out in a three-electrode configuration with a Swagelok-type cell, using either as obtained expanded graphite or cobalt oxide-coated expanded graphite as the working electrode, a commercial activated carbon fiber as the counter electrode, Hg/HgO (1 M NaOH) as the reference electrode and aqueous 6 M KOH as the electrolyte. Cobalt oxide-coated cathodically expanded graphite was prepared by synthesizing cobalt oxide nanosheets in the confined 2D space of lamellar reverse micelles as reported elsewhere [36] but here in the presence of the cathodically expanded graphite. Specifically, 200 mg of Pluronic P123 were dissolved in 17.5 mL of a mixed ethanol/water (33/2, v/v) solvent under stirring. Subsequently, 250 mg of cobalt (II) acetate tetrahydrate, 70 mg of hexamethylenetetramine and 50 mg of cathodically expanded graphite were added to the resulting mixture. After 15 min, 13 mL of ethylene glycol were poured into the suspension. After 30 min of continuous stirring, the mixture was allowed to statically age for 24 h. The aged suspension was then transferred to a Teflon-lined autoclave (capacity: 40 mL) and heat-treated at 170 ºC for 2 h. The resulting slightly greenish solid product was thoroughly washed by repeated cycles of centrifugation (2000 g for

20 min, J.P. Selecta Meditronic centrifuge in 30 mL tubes) and re-suspension first in water and then in ethanol (3 cycles for each solvent), and finally dried at room temperature under a vacuum. The amount of cobalt oxide incorporated to the cathodically expanded graphite was determined from the difference between the elemental analyses of expanded graphite alone and combined with cobalt oxide (LECO Truspec Micro CHN microanalyses apparatus with a LECO Truspec Micro O accessory for direct O determination). For the electrochemical charge storage tests, the working electrode was prepared by pressing uncoated or cobalt oxide-coated expanded graphite powder onto circular graphite foil pieces (~1 cm in diameter). Typical loadings onto the graphite foil support were ~1 mg cm^{-2}. The counter electrode was obtained in the form of a paste that incorporated, in addition to the activated carbon fiber, polytetrafluoroethylene as a binder and carbon black as a conductive additive, in a weight ratio of 90:5:5. A circular piece (~1.3 cm in diameter) of nylon membrane filter (0.45 μm of pore size, from Whatman) was used as the electrode separator. Before the cell was assembled, the working and counter electrodes as well as the separator were individually soaked in 6 M KOH and vacuum-degassed. Prior to the measurements, the assembled cell with the electrolyte was also vacuum-degassed. The measurements were carried out in a VSP potentiostat (Bio-Logic Science Instruments), recording cyclic voltammograms at different voltage scan rates, and galvanostatic charge/discharge curves at different current densities. Electrochemical impedance spectra were also recorded for the fully discharged cell in the frequency region between 100 kHz and 10 mHz at a voltage amplitude of 10 mV.

3. Results and discussion

3.1. Screening of efficient electrolytes for the cathodic exfoliation of graphite in water

The electrochemical exfoliation of graphite in aqueous medium to afford graphene nanosheets is usually accomplished under anodic conditions, whereby the graphite electrode is efficiently delaminated upon application of a positive voltage in the presence of a proper electrolyte (typically, a sulfate-based one) [10,11]. This process is believed to be driven, at least in its early stages, by the oxidation of graphite at edges, grain boundaries and other defects, which in turn is induced by highly reactive oxygen radicals generated from the oxidation of water molecules at the graphite anode [37,38]. In particular, the oxidative attack of graphite edges and their subsequent decoration with hydrophilic oxygen functional groups can be expected to lead to a local increase in the interlayer spacing, thus facilitating the intercalation of hydrated anions from the electrolyte (i.e., anions surrounded by a bound shell of water molecules) into the interlayer galleries of the material. These intercalated species could then act as a sort of molecular wedge to trigger the separation of the constituting graphene sheets from one another (i.e., to trigger their exfoliation), probably assisted by the electrolytic decomposition of the water molecules into gaseous products (e.g., O_2).

On the other hand, such a course of events is not expected to occur in a prospective cathodic exfoliation with an aqueous electrolyte, because in this case water-derived oxygen radicals will not be generated at the graphite cathode under the applied reducing conditions. As a result of the lack of oxidative attack, the graphite edges will remain unexpanded and hydrophobic, therefore hindering the intercalation of hydrated cations and so the electrode exfoliation. A possible way to circumvent this issue and allow cathodic exfoliation in water could be to use graphite materials with pre-expanded edges and interlayer voids, which would expedite the entrance of ionic species from the electrolyte without the need to resort to oxidation processes. To this end, graphite foil appeared to be a good candidate [39]. Indeed, prior studies have indicated that anodic

intercalation and exfoliation processes are promoted in graphite foil compared to other graphite types, such as highly oriented pyrolytic graphite (HOPG) or graphite rod, powder and flakes [14,39] suggesting that similar effects could be in place for cathodic processes. As will be discussed and rationalized below, the choice of graphite foil as the electrode material turned out to be one of the critical factors for the success of cathodic exfoliation in water.

As potential electrolytes for the exfoliation experiments, we selected a number of ammonium-based salts, where the ammonium cation was derivatized with different alkyl or phenyl groups and the counterion was typically a halide (Cl^- or Br^-). We note that at least in organic solvents, several ammonium-based cations are known to intercalate and exfoliate graphite efficiently under cathodic potentials [21–23,30,40]. Table 1 lists the names, acronyms used and chemical structures of the tested species. To provide an initial, quantitative proxy for the ability of these electrolytes to intercalate/exfoliate the graphite electrode, we carried out benchmark experiments whereby a piece of graphite foil of fixed dimensions ($55 \times 30 \times 0.5$ mm^3) was subjected to cathodic treatment (bias voltage: -10 V) for 2 h in a two-electrode setup using Pt foil as the counter electrode in an aqueous solution of a given electrolyte at a certain molar concentration (see Experimental section for details of the treatment and Table 1 for the molar concentrations tested with each electrolyte). In many cases, the graphite cathode was seen to progressively swell and expand upon application of the negative potential, to an extent that depended on the particular electrolyte and electrolyte concentration tested. To illustrate this point, Fig. 1a shows digital photographs of the cross-section of graphite foil pieces before (left) as well as after cathodic treatment in 0.3 M PhTMACl (middle) and 0.3 M HTMABr (right). Upon completion of the electrolytic step, the expanded products were collected, thoroughly washed with water to remove remnants

of the ammonium-based salt, dried under reduced pressure and finally the resulting fluffy, low density (30–45 mg cm^{-3}) powders were weighed to estimate the efficiency (yield) of the expansion process. Comparison of field-emission scanning electron microscopy (FE-SEM) images of the starting graphite foil, which appeared mostly planar and featureless on the millimeter scale (Fig. 1b), with those recorded for the expanded material obtained with an efficient electrolyte, such as 0.3 M HTMABr (Fig. 1c and d), revealed that the cathodic treatment led to a dramatic expansion of micrometer-sized graphite particles (presumably along the *c* axis of their atomic lattice) to give worm-like objects (Fig. 1c). Closer inspection of the latter indicated that they were made up of thin, corrugated sheets separated by micrometer- to nanometer-wide voids (Fig. 1d). Such a morphology was very similar to that previously reported in efficient processes of anodic [15,14,37,41,42] and cathodic (in organic solvent [18,21,23]) delamination of graphite to give graphene nanosheets, suggesting that a satisfactory exfoliation can also be attained in aqueous medium under cathodic conditions. This point will be corroborated further below.

Table 1. Name, acronym, chemical structure and the different molar concentrations assayed for each ammonium-based salt tested as an electrolyte in the cathodic exfoliation of graphite. The corresponding yields of expanded graphite obtained after 2 h of electrochemical treatment, calculated as the weight of expanded graphite relative to the weight of the starting graphite foil piece, are also indicated.

Electrolyte (acronym)	Structure	Conc (M)	Yield of expanded graphite (wt%)
Ammonium chloride (ACl)	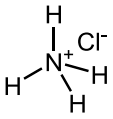	0.02 0.1 0.3	0 0 0
Trimethylamine hydrochloride (TMAHCl)	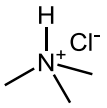	0.02 0.1 0.3	0 0 0.5
Tetramethylammonium chloride (TMACl)	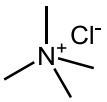	0.02 0.1 0.3	2.0 8.7 15
Tetraethylammonium chloride (TEACl)	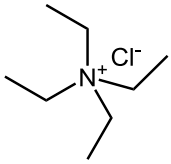	0.02 0.1 0.3	3.3 12 28
Tetrapropylammonium chloride (TPACl)	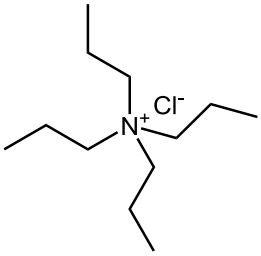	0.02 0.1 0.3	7.0 13 44
Tributylamine hydrochloride	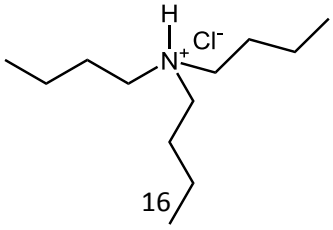	0.02	0

(TBAHCl)		0.1	0
		0.3	0
Tributylmethylammonium chloride (TBMACl)	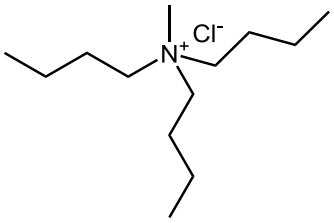	0.02	5.3
		0.1	12
		0.3	25
Tetrabutylammonium chloride (TBACl)	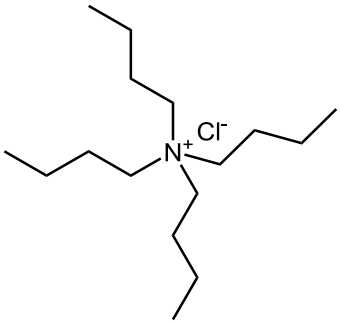	0.02	5.7
		0.1	13
		0.3	33
Hexyltrimethylammonium bromide (HTMABr)	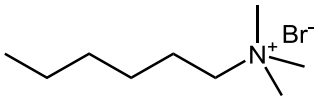	0.02	0.4
		0.1	18
		0.3	46
Octyltrimethylammonium bromide (OTMABr)	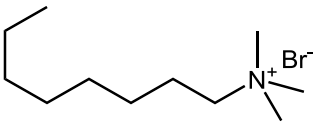	0.02	1.8
		0.1	13
		0.3	26
Dodecyltrimethylammonium bromide (DDTMABr)	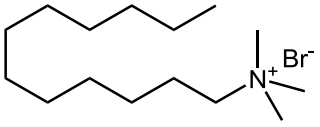	0.02	2.9
		0.1	8.0
		0.3	13
Hexadecyltrimethylammonium	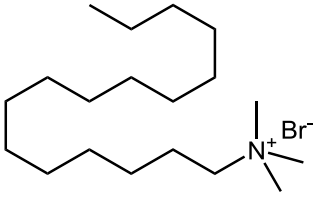	0.02	0

bromide		0.1	4.6
(HDTMABr)		(*)	
Phenyltrimethylammonium	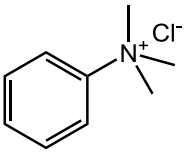	0.02	2.2
chloride		0.1	2.8
(PhTMACl)		0.3	14
Benzyltrimethylammonium	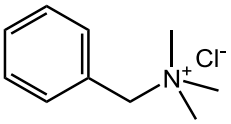	0.02	0.7
chloride		0.1	7.5
(BzTMACl)		0.3	25

(*) The solubility of HDTMABr lies below 0.3 M.

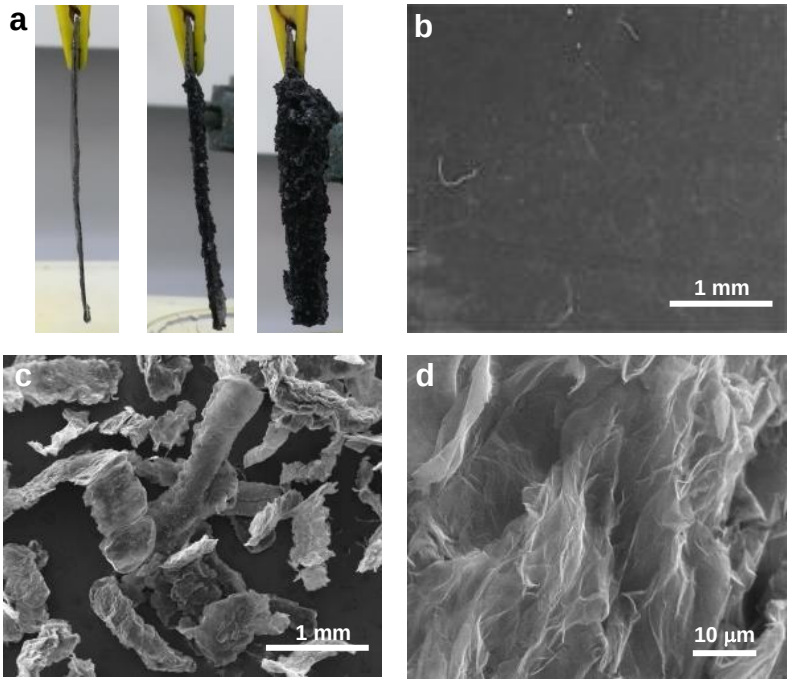

Figure 1. (a) Digital photographs of the cross-section of graphite foil pieces before (left) and after cathodic treatment in 0.3 M PhTMACl (middle) and 0.3 M HTMABr (right). **(b-d)** Typical FE-SEM images of **(b)** the starting graphite foil and **(c,d)** the

cathodically expanded material obtained from it after cathodic treatment for 2 h using 0.3 M HTMABr as the electrolyte.

The yield of expanded product, calculated as its weight relative to the weight of the starting graphite foil piece, was taken as a quantitative measure of the efficiency of the cathodic treatment, and the values determined for the tested electrolytes at different concentrations are given in Table 1. First of all, we note that for almost any given electrolyte the yield of expanded material tended to increase with the electrolyte concentration, which was a clear indication of the central role played by these ionic species in the expansion of the material. Second, large differences in yield values were noticed between the different electrolytes. In particular, some of the tested species, i.e. ACl, TMAHCl and TBAHCl, gave very small or even virtually negligible yields. We interpret this result to be related to the fact that one or more hydrogen atoms were directly connected to the N^+ site in the corresponding cation. This type of cation should be readily reduced at the graphite cathode to afford a stable, electrically neutral product and molecular hydrogen (e.g., $2NH_4^+ + 2e^- \rightarrow 2NH_3 + H_2$ in the case of ACl) [43,44]. If the cation is reduced promptly to a neutral species after contacting the electrode, it will lose its electrophoretic mobility and hence most of its ability to intercalate the graphite material. As a result, no or very little expansion of the latter should take place. On the other hand, the electroreduction of cations without bound hydrogen atoms (i.e., with only alkyl or phenyl moieties bound to the N^+ site) can be expected to be a less likely event, so that their intercalation into the graphite electrode would not be so much hampered by the loss of electrophoretic mobility. Such an interpretation was supported by the observation that when the TMAHCl and TBAHCl electrolytes were replaced by TMACl and TBMACl, respectively, which only differ from the former in the

substitution of a methyl group for the N^+-bound hydrogen, very substantial yields of expanded product could be attained.

The results collected in Table 1 also provided some insight into the effect that the size of the alkyl groups appended to the N^+ site of the electrolyte has on its ability to induce expansion of the graphite cathode. In principle, larger alkyl chains should be more conducive to an efficient separation of neighboring sheets in the graphite electrode upon cation intercalation, as a stronger wedge effect can be expected for bulkier species. However, the ability of cations from the electrolyte to enter the interlayer space of graphite in the first instance should be limited by their size, both in a direct way (i.e., if the cations are too large, steric effects should prevent them from penetrating the interlayer spaces) and indirectly through constraints on their electrophoretic mobility, which is largely determined by their charge/mass ratio [17]. For instance, the mobility of tetraalkylammonium cations in water is known to decrease with the alkyl chain length (i.e., methyl > ethyl > propyl > butyl) [45,46]. Based on these considerations, it can be anticipated that the intercalation and expansion of the graphite cathode should be most effective with ammonium-based cations of a certain intermediate size. This conclusion was substantiated by comparing the yields of expanded material within specific sets of the electrolytes from Table 1. More specifically, for the case of the tetraalkylammonium-based electrolytes with the four alkyl chains in the cation being identical (i.e., TMACl, TEACl, TPACl and TBACl), the measured yields clearly increased in the order TMACl < TEACl < TPACl, but the performance of their butyl-based counterpart (TBACl) was similar or even lower (at the higher electrolyte concentration) than that of TPACl. Indeed, TPACl turned out to be a very efficient electrolyte, boasting yields up to 44 wt% (i.e., almost half of the graphite foil piece was converted to expanded product).

A similar behavior was noticed for the series of electrolytes with the cation comprising three methyl groups and a fourth alkyl chain of variable length, namely, methyl, hexyl, octyl, dodecyl or hexadecyl (i.e., TMACl, HTMABr, OTMABr, DDTMABr and HDTMABr). For these alkyltrimethylammonium species, the highest expansion efficiency was attained with the hexyl-based cation and was similar to that of TPACl (e.g., a yield of 46 wt% at 0.3 M HTMABr), declining significantly for cations with longer chains. Likewise, replacing the alkyl group in the ammonium cation with an aryl moiety was detrimental to its ability to intercalate and expand the graphite cathode. This can be seen by comparing the yields of expanded product obtained with HTMABr (hexyl group) to those afforded by PhTMACl (phenyl group), where both groups possess the same number of carbon atoms (and thus the cations have very similar molecular weights) but the latter gave substantially lower yields. As a tentative explanation for such a result, it can be argued that the phenyl moiety forces the cation to take on a relatively flat conformation upon intercalation into graphite, in order to maximize its interaction with the carbon surface. With a flat configuration, the ability of the intercalated cation to act as a molecular wedge and expand the graphite cathode would be decreased. This interpretation was supported by the observation that when the phenyl group was replaced by a benzyl moiety (i.e., the BzTMACl electrolyte), which can be expected to hinder the adoption of flat configurations by the cation, higher yields of expanded material were attained.

Nevertheless, we note that the ability of some of the alkyltrimethyl-based electrolytes to intercalate and expand the graphite cathode could be affected by their tendency to form micelles above a certain concentration (referred to as the critical micelle concentration, or cmc), giving rise to more complex behaviors. This should be particularly the case for the two longer-chain species (DDTMABr and HDTMABr),

which are broadly used cationic surfactants and have cmc values lying below the range of concentrations tested here for the cathodic expansion experiments (see cmc values in the Experimental Section). More specifically, at concentrations above the cmc threshold, the number of surfactant monomers in the solution (i.e., those molecules that remain as stand-alone, non-associated entities) is known to be approximately invariant with respect to surfactant concentration, whereas the number of molecules associated in micelles increases monotonically with surfactant concentration [33]. It is reasonable to assume that the monomeric entities contribute most effectively to the expansion of the graphite cathode, as they are readily available cations for intercalation. On the other hand, the actual contribution of surfactant cations assembled into micelles to the graphite expansion is much less obvious: while surfactant micelles are dynamic objects, with individual molecules continuously incorporating to and detaching from the assembly, intercalation of a molecule (cation) from a micelle into graphite should involve overcoming first a certain barrier associated to its detachment from the micelle. As a result, the micelle-assembled cations should be less available for intercalation than their stand-alone, monomeric counterparts. Consequently, at least part of the mediocre to poor performance of DDTMABr and HDTMABr as electrolytes for the cathodic expansion of graphite (Table 1) should be ascribed to this effect. Such a situation was not believed to be in place in the case of the relatively shorter chain alkyltrimethyl-ammonium cations (octyl and hexyl), since their corresponding cmc values were above the tested range of electrolyte concentrations (see cmc values in the Experimental Section). Nonetheless, the extent to which micellization of DDTMABr and HDTMABr limited their ability to intercalate and expand the graphite cathode is currently unknown and its determination lies beyond the scope of the present work.

3.2. Physicochemical characteristics of the cathodically exfoliated graphenes

While some of the tested aqueous electrolytes (e.g., HTMABr and TPACl) demonstrated a good ability to intercalate the graphite cathode and give high yields of expanded product, the actual amount as well as the characteristics of graphene nanosheets that could be extracted from the latter were a priori unknown and needed to be determined. Nanosheet extraction from electrochemically exfoliated graphites is typically accomplished through a sonication step in proper solvents [10,47]. To this end, a certain amount of expanded material was transferred to a solvent medium, where it was subjected to mild sonication to separate loosely attached, thin nanosheets from poorly exfoliated, relatively thick platelets, and finally either centrifuged at 50 g for 20 min or allowed to stand undisturbed overnight, with the resulting supernatant (dispersion) being collected for further studies and the sediment being discarded (see Experimental section for details). Fig. 2a shows a digital photograph of several successful dispersing solvents, where the supernatant material could be stably suspended for days to weeks, as denoted by their dark grey or black tone. These solvents included *N*-methyl-2-pyrrolidone, *N*-vinyl-2-pyrrolidone, *N*-ethyl-2-pyrrolidone, *N*,*N*-dimethylformamide, pyridine, 1,3-dioxolane, dimethyl sulfoxide, ethlylene glycol and water with the non-ionic surfactant Pluronic P123 (triblock copolymer). Other tested solvents that turned out to be ineffective for dispersion comprised pure water (as could be expected for low-oxidized nanosheets), water/isopropanol mixtures and ethanol. Representative UV-vis absorption spectra of the material suspended in some successful solvents, specifically, ethylene glycol (red trace), and water /P123 (blue trace), are presented in Fig. 2b. It is dominated by a strong absorption peak located at about ~270 nm, together with substantial, slowly decreasing absorbance at longer wavelengths. These features are known to be characteristic of graphitic, sp^2-based carbon nanostructures with limited oxidation, including pristine

graphene and well reduced graphene oxide nanosheets, but not (unreduced) graphene oxide [39,48,49]. In particular, the peak at ~270 nm has been ascribed to $\pi \rightarrow \pi^*$ transitions in electronically conjugated domains of carbon materials with sizes larger than those typical of the conjugated domains in graphene oxide (i.e., larger than a couple of nanometers) [39,50]. The UV-vis spectra of the rest of the successful solvents are not shown as their absorption saturates the signal in the UV range, thus precluding the observation of graphene characteristic adsorption peak at ~270 nm.

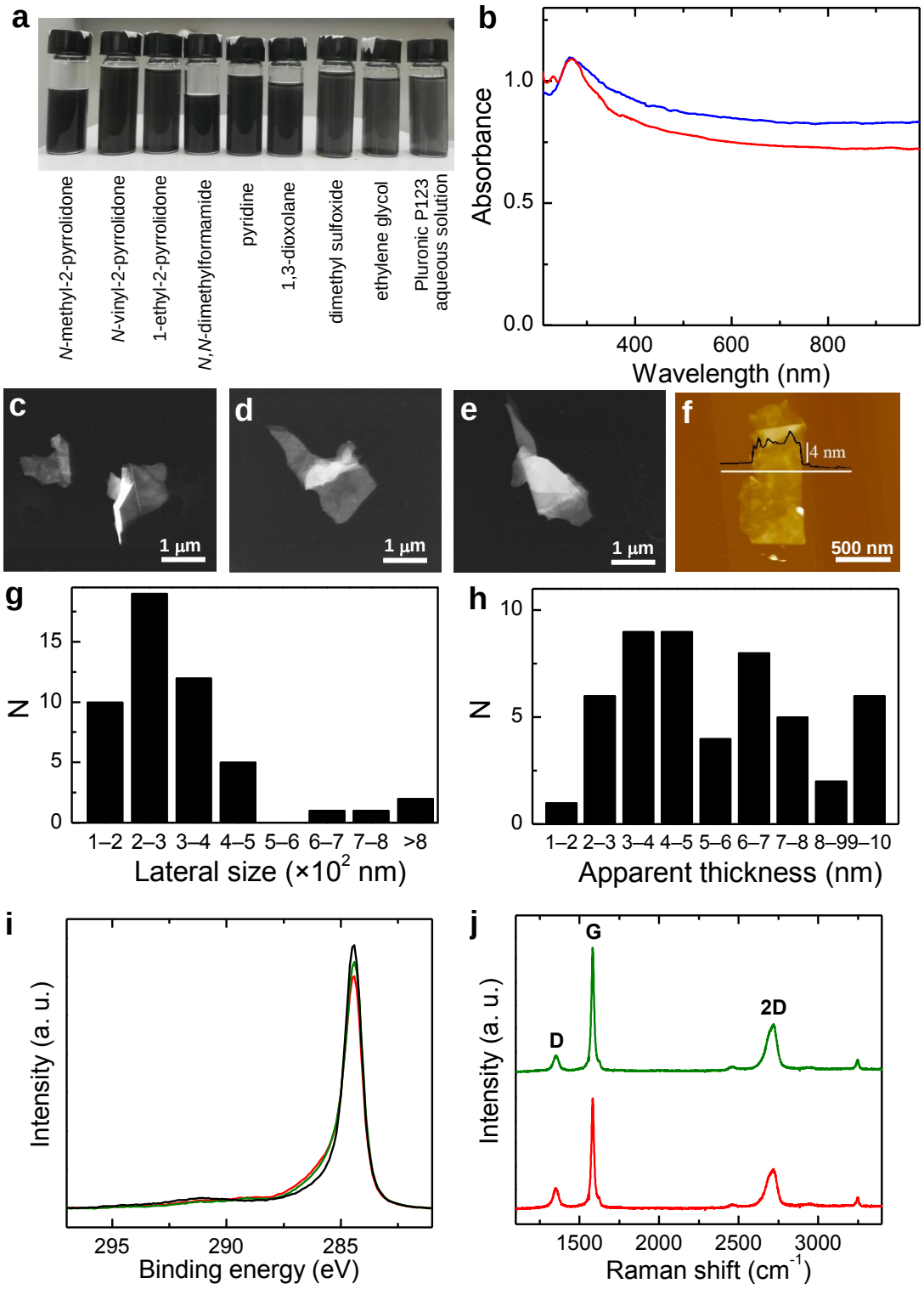

Figure 2. Physicochemical characterization of the cathodically exfoliated graphenes isolated by ultrasonication of the expanded product in solvent media: **(a)** Digital picture of graphene dispersions in different solvents. From left to right: *N*-methyl-2-pyrrolidone, *N*-vinyl-2-pyrrolidone, *N*-ethyl-2-pyrrolidone, *N*,*N*-dimethylformamide,

pyridine, 1,3-dioxolane, dimethyl sulfoxide, ethylene glycol and water with the non-ionic surfactant Pluronic P123 (0.5 wt%). **(b)** UV-vis absorption spectra of graphene dispersions obtained with 0.3M HTMABr in ethylene glycol (red trace), and water /P123 (blue trace). **(c-e)** Representative STEM images recorded for cathodic graphene flakes. **(f)** Typical AFM image of graphene flakes deposited onto HOPG substrate from their dispersion. A representative line profile (black line) taken along the marked white line is shown overlaid on the image. Histograms of **(g)** lateral size and **(h)** apparent thickness of graphene flakes derived from a pool of 50 flakes measured from AFM images. **(i)** Background-subtracted, normalized high resolution XPS C 1s core level spectra recorded for graphene obtained with 0.3 M HTMABr (red trace) and 0.3 M TPACl (green trace). The spectrum of the starting graphite foil has been added as a reference (black trace). **(j)** Raman spectra of graphene obtained with 0.3 M HTMABr (red trace) and with 0.3 M TPACl (green trace). The main bands have been labeled for clarity.

The physicochemical characteristics of the solvent-dispersed objects (e.g., lateral size and thickness, presence of structural defects and chemical composition) were analyzed by both microscopic and spectroscopic techniques. Direct evidence of the efficient generation of graphene nanosheets from the aqueous cathodic process was gathered by scanning transmission electron microscopy (STEM) and atomic force microscopy (AFM). Figure 2c-e shows typical STEM images recorded for graphene flakes obtained using 0.3 M HTMABr as. In all cases, the observed flakes exhibited an irregular polygonal shape with typical lateral sizes of several hundreds of nanometers, as shown in the histogram of flake lateral size in Fig. 2g. The apparent thickness of the flakes derived from representative AFM height profiles ranged from a few to several nm

(Fig. 2f and 2h). However, detailed inspection of the AFM images revealed that the flakes were decorated by discrete features about 1 nm high, which could be ascribed to remnants of electrolyte and/or organic solvent molecules that remain adsorbed on the graphene surface despite the washing. The detection of small amounts of nitrogen (<1 at%) by X-ray photoelectron spectroscopy (XPS) analysis of paper-like films prepared by filtration of the graphene dispersions (see Fig. S1a of the Supplementary material) provided further evidence of the presence of electrolyte and/or organic solvent molecules adsorbed on their surface. Indeed, this effect has been previously reported for cathodically exfoliated graphite obtained with ammonium-based salts in organic medium [21]. It was thus reasonable to assume that the measured apparent thickness of the flakes included a contribution of up to about 2 nm (i. e., ~1 nm from each face of the flake) from adsorbed electrolyte/organic solvent. Consequently, the actual thickness of the flakes would be below 8 nm, typically comprising a few to several graphene layers. Chemical analysis by XPS of the graphene flakes processed into films revealed that carbon was the dominant element, although some amount of oxygen and nitrogen, as mentioned above, was also found (see Fig. S1a of the Supplementary material). The O/C atomic ratio was 0.05–0.08, similar to the values reported for prior cathodically exfoliated graphenes obtained in organic media [19,21]. These values are lower than those usually found for anodically exfoliated graphite or reduced graphene oxide, with O/C atomic ratio values typically ranging between 0.10 and 0.20 but much higher than those of pristine graphene flakes derived from direct exfoliation routes (O/C ratios 0.01) [12]. Fig. 2i shows high resolution C 1s core level spectra for graphene obtained with 0.3 M HTMABr (red trace) and 0.3 M TPACl (green trace). For comparison purposes, the corresponding spectrum for the starting graphite foil is also shown (black trace). As clearly seen, the difference between the spectra of the cathodically exfoliated graphenes

and the starting graphite are marginal (see difference spectra in Fig. S1b of the Supplementary material). Indeed, the C 1s band for the cathodically exfoliated graphenes was sharp and centered at ~284.6 eV (C=C structures in non-oxidized graphitic domains), and displayed only a minor contribution from oxidized species (e. g., hydroxyl or epoxide C-O groups) centered at ~286.5 eV [39]. These results corroborated that the cathodic graphenes obtained in aqueous medium were oxidized only to a rather limited extent.

The structural quality of the cathodic graphenes was evaluated by Raman spectroscopy, as illustrated in Fig. 2j for materials obtained with 0.3 M HTMABr (red trace) and 0.3 M TPACl (green trace) as electrolytes. The spectra were dominated by three bands: the G band characteristic of graphite/graphene materials (~1582 cm^{-1}), the defect-related D band (~1350 cm^{-1}) and its overtone, the 2D band (~2700 cm^{-1}) [51]. The integrated intensity ratio of the D and G bands (I_D/I_G ratio), which is widely adopted as a quantitative measure of the amount of defects present in graphitic structures [51], yielded values of 0.2–0.3 for the cathodically exfoliated graphenes. These values are comparable to, or even lower than, those usually reported for graphenes obtained by direct liquid-phase exfoliation of graphite. Although such I_D/I_G ratios were significantly larger than that of the starting graphite foil (~0.03), they are not thought to arise from a greater number of basal plane defects in the exfoliated graphene flakes, but from the relatively small lateral dimensions of the flakes. Given that the diameter of the Raman laser spot (a few micrometers) was larger than the typical flake size (see Fig. 2c–f and discussion above), the flake edges must have contributed substantially to the intensity of the defect-related D band [52,53].

Taken together, the characterization results allow concluding that the dispersions obtained via aqueous cathodic exfoliation were comprised of few- to several-layer

graphene flakes that largely retained the chemical and structural integrity of their parent material. Such high structural quality and limited oxidation was expected to imply the retention of high electrical conductivity. Indeed, the conductivity of films obtained by vacuum-filtration of the present cathodic graphene dispersions obtained using, e. g., 0.3 M HTMABr as the electrolyte was 1.5×10^4 S m^{-1}. This figure compared favorably with the values previously reported for graphene films obtained by direct exfoliation of graphite via ultrasonication in organic solvents or water-surfactant systems (~2×10^2–5×10^4 S m^{-1} [35,52–55]) and was similar to the values obtained beforehand for films of high-quality, low-oxidized anodic graphene obtained with oxidation-preventing electrolytes or electrolyte additives (~1×10^4 –4.6×10^4 S m^{-1} [16,17,38]).

3.3. Overall yield of the exfoliation process and relevance of the starting graphite type

The overall yield of graphene nanosheets produced with the best-performing aqueous electrolytes (i.e., the mass of graphene extracted from the expanded material relative to the mass of the starting graphite foil piece) was estimated by determining the concentration of the corresponding dispersions in a good solvent such as *N*-methyl-2-pyroolidone. Dispersion concentrations were assessed following previously reported protocols based on the use of UV-vis absorption spectroscopy (Lambert-Beer law [17,35]). For many electrolytes, roughly one third to one half of the mass of the expanded product could be extracted as graphene nanosheets, implying that the overall graphene yield was about one third to one half of the corresponding yield of expanded material. This was particularly the case of the best electrolytes, namely, TPACl and HTMABr, which boasted overall yields of ~15–20 wt%. It is important to note that the yield of expanded product and thus the overall graphene yield were highly dependent on the thickness of the graphite foil piece used in the experiments, thinner foils affording

higher yields of expanded material. The yields of expanded product collected in Table 1 were obtained with ~500 μm thick graphite foil, whereas in many instances in the literature substantially thinner foils (e.g., between 100 and 250 μm) have been used for electrochemical exfoliation experiments (both anodic and cathodic [16,19,25,32,37,56]). Indeed, carrying out the cathodic treatment in 0.3 M TPACl or HTMABr with ~70 μm thick foil pieces led to yields of expanded product close to 100 wt%, and thus to overall graphene yields of ~40–50 wt%. These overall yields were commensurate with, or even better than, the graphene yields previously reported for the cathodic exfoliation of different types of graphite (foil, rod, powder, etc) in organic solvents [18,24,26,27,57–59] indicating that the present water-based cathodic approach is competitive with those implemented in non-aqueous media. The increase in yield obtained by departing from thinner foils could also be attained using ~500 μm thick graphite foil by repeating the process in consecutive steps. Indeed, the foil did not lose its integrity after cathodic expansion and could be re-used as cathode after gently scrapping the fraction that was expanded from its surface. In each consecutive step, a similar amount of graphite was detached and expanded from the graphite foil. Thus, as could be expected, the yield of expanded product became nearly 100% after 2 steps at 0.3 M TPACl and 0.3 M HTMABr, after 3 steps at 0.3 M TBACl and 0.3 M TEACl, and after 4 steps at 0.3 M BzTMACl.

As briefly noted above, a critical issue for the successful attainment of graphene through cathodic exfoliation in water was a proper choice of the graphite type to be used as an electrode. While substantial amounts of expanded product and then graphene nanosheets could be generated with certain electrolytes and graphite foil as the cathode (Table 1), the same was not true when graphite foil was replaced by other types of graphite, such as graphite rod or HOPG. In these cases, almost no expansion of the

cathode was observed even if using the best-performing electrolytes (for HOPG, a very slight expansion could be noticed), so that graphene nanosheets could not be extracted in any significant quantities. We believe the ultimate origin of such a discrepancy between graphite foil and other graphite types to be in the different packing configurations of the graphene layers in the materials. For HOPG, graphite rod and other graphite varieties (powder, flakes), the graphene layers are very tightly stacked onto each other, leaving essentially no interlayer voids or openings [39]. In the absence of oxidation processes at the graphite electrode during the electrolytic treatment, which are only expected to occur under anodic conditions, the interlayer spaces adjacent to the graphite edges should remain mostly hydrophobic and unexpanded, thus preventing the entry of hydrated cations from the electrolyte and thus the electrode expansion (Fig. 3a).

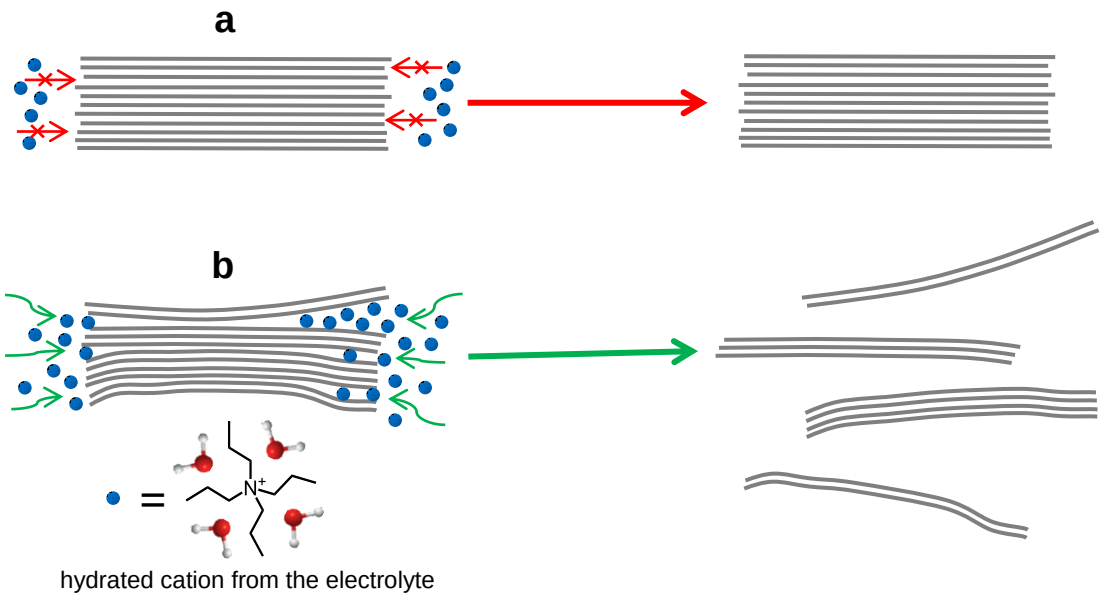

Figure 3. Schematic of the cathodic exfoliation process for **(a)** graphite with tightly stacked graphene layers, such as graphite powder, flakes, rod, etc. and **(b)** graphite containing local areas with expanded interlayer spacing, such as graphite foil. In (a),

hydrated cations from the electrolyte are not able to enter the interlayer spaces, as the latter remain hydrophobic and unexpanded due to the absence of oxidizing conditions in the electrolytic treatment. As a result, no expansion and exfoliation of the material is attained. In (b), pre-formed interlayer openings and voids in the graphite material facilitate the entry of hydrated cations, then triggering its expansion and exfoliation.

On the other hand, graphite foil is known to possess a large number of nanometer-sized interlayer voids and packing imperfections, i.e., local areas with expanded interlayer spacing, which arise from its production process (roll compaction of expanded graphite particles [39]). Indeed, FE-SEM images of the surfaces of HOPG and graphite foil observed at an angle of ~ 45° in respect of the basal plane (see Fig. S2 in the Supplementary material) reveal, respectively, the absence and presence of voids and imperfections. In particular, the interlayer voids located adjacent to graphite edges should act as selective entry points and facilitate the initial intercalation of a number of hydrated cations from the electrolyte (Fig. 3b). The latter would then behave as a sort of advance party, playing the role of a molecular wedge and triggering a further expansion of the interlayer spacing at increasing distances from the edges into the graphite particle. In turn, this process should favor the subsequent intercalation of more hydrated cations, which would continue cleaving the layers to finally give expanded products from which graphene nanosheets can be readily extracted. The reduction of the water molecules that hydrate the cations would generate hydrogen and the gas pressure built-up in the interlayer spaces could contribute as well in some extent to the expansion. Overall, it can be concluded that a pre-requisite for the successful exfoliation of graphite in water under both anodic and cathodic conditions is the presence of expanded edges that facilitate the intercalation of hydrated ions. However, whereas expanded edges can be

generated *in situ* under anodic conditions as a result of built-in oxidation processes [11,37], they have to be pre-formed by some means for cathodic exfoliation, for instance, by applying a proper pre-expansion step to the graphite material, as was the case of graphite foil. We also note that the need to use this type of graphite should not constitute a significant problem with a view to the industrial implementation of cathodic exfoliation in water for the production of high quality graphene. Graphite foil is manufactured annually by the ton as a modestly priced commodity (less than U.S. $0.1 per gram, compared to about U.S. $100 per gram for HOPG), which should contribute to the affordability of the aqueous cathodic route.

2.4. Application of cathodically exfoliated graphene as sorbent in oil absorption and electrochemical energy storage

The high-quality, low-oxidized, and electrically conductive graphene obtained here by aqueous cathodic exfoliation could find use, e. g., as a sorbent in water/oil remediation, where hydrophobicity is a requisite, or as an electrode for energy storage, where a high electrical conductivity is needed. A large specific surface area would be an additional requirement for both applications that graphene-based materials could in principle fulfill. Among our materials, those subjected to sonication after cathodic expansion would in principle display higher exposed surface areas in liquid media. However, when these well-separated graphene nanosheets are removed from their dispersing solvent or when the (non-sonicated) cathodically expanded graphite materials are removed from their electrolytic and washing media to handle them as bulk solid products for practical uses, they tend to re-stack into more compact configurations, with the subsequent decrease in surface area and performance in such uses [60]. To alleviate this issue, proper assembling strategies must be put in place, which frequently involve

the construction of three-dimensional structures with the aid of components other than graphene [61]. Here, we have investigated two such protocols for the present cathodic graphene in the context of its use as a sorbent for oils/organic solvents and as an electrode for energy storage (supercapacitors). Fig. 4a shows the sorption capacity of as-expanded (non-sonicated) materials obtained via cathodic exfoliation of graphite using 0.3 M HTMABr (red bars) and 0.3 M TPACl (green bars) towards several organic solvents and oils, namely, toluene, heptane, dodecane, tetrahydrofuran, acetone, chloroform, olive oil and pump oil. As expected from their hydrophobic nature, these materials were good sorbents for such liquids, with measured sorption capacities ranging between ~8 and 20 g/g, comparable to those reported for light weight graphene-based sorbents of similar density (30–45 mg cm^{-3} [14]) (see Table S1 in the Supplementary material for a comparative list). Nevertheless, it is noteworthy that the much simpler and faster preparation of the present materials constitutes an asset over those prior graphene-based sorbents. To improve these sorption figures with cathodic graphene, though, it is clear that macroscopic structures of a lower density must be used. To this end, we resorted to commercial melamine foam (density: ~8–10 mg cm^{-3}) as a scaffold that was coated with a thin layer of graphene nanosheets [62]. Coating was accomplished by repeatedly soaking the foam into a (sonicated) dispersion of cathodic graphene nanosheets in pyridine and drying at moderate temperature, giving rise to graphene loadings on the foam of up to 4 mg cm^{-3} (see Experimental section for details). This was considered as the optimal loading, that is, the minimum needed to avoid absorption of water by the foam. Fig. 4b shows digital photographs of the starting melamime foam (white dices) and the graphene-coated one (blackish dices) after casting droplets of acetone and water with yellow and magenta dye, respectively, to facilitate observation of their fate. The neat, non-coated melamine foam, which was originally

both hydrophilic and oleophilic, and thus would not be fitted as sorbent for water remediation, as it would indiscriminately adsorb water and pollutant, became highly hydrophobic after coating with graphene. Indeed, the water contact angle for the graphene-coated material was determined to be ~120° (inset to bottom panel of Fig. 4b). FE-SEM imaging provided insight into the structural origin of the observed change: the starting (hydrophilic) surface of the foam (Fig. 4c) became largely covered with the (hydrophobic) graphene nanosheets after dip-coating (Fig. 4d). These results indicate that the graphene-coated foam can be used as a selective sorbent for, e. g., removing oil spills from water, as illustrated by the series of successive (from left to right) digital photographs shown in Fig. 4e, where the oil phase originally floating on water was removed by dipping the graphene-coated foam. The measured sorption capacities of the graphene-coated foam towards the different solvents ans oils are given in Fig. 4f, with typical values ranging between 60 and 150 g/g, i. e., 3 to 10 times larger than those determined for by the as-expanded material (compare Figs. 4a and f). This improvement must come from the lower density (~12–14 mg cm^{-3}) of the former sorbent. Another advantage of the graphene-coated foam over the as-obtained powdery solid lies in its easier handling. Indeed, as seen in the digital photographs in Fig. 4e, oil contamination could readily be removed from water just by dipping the coated foam sorbent into the liquid for a few seconds. The regeneration of the foam could be performed very conveniently as well, just by squeezing it and gathering the desorbed liquid on absorbent paper. Furthermore, the sorption capacity for the oils after ten sorption/desorption cycles was retained to a large extent, as indicated by the re-usability tests gathered in Fig. 4g. We note that the ability of the cathodic graphene-coated foam to retain its oil sorption capacity after repeated use was much better than that of previously reported melamine foam coated with graphene derived from chemically

expanded graphite, where an ~80% decrease in oil sorption capacity was measured during the first few cycles [62], thus highlighting the practical advantage of the present materials. These re-usability tests also provided indirect evidence of the stability of the sorbents, and thus of the durability and strength of the adhesion between graphene coating and melamine foam.

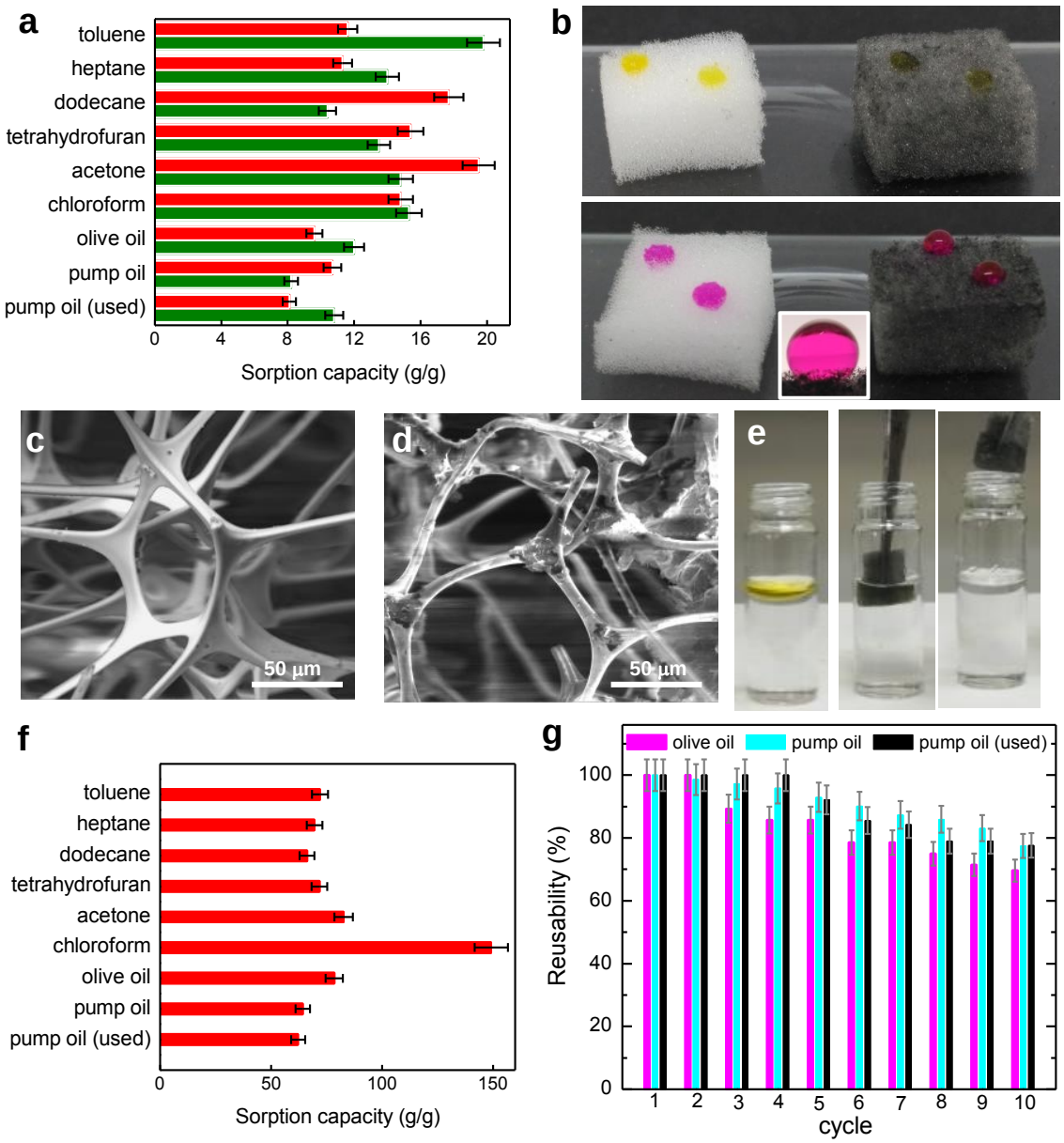

Figure 4. (a) Sorption capacity for different organic solvents and oils of as-expanded graphite materials obtained via cathodic exfoliation of graphite foil using 0.3 M HTMABr (red bars) or 0.3 M TPACl (green bars) as the electrolyte. **(b)** Digital pictures of droplets of acetone (top) and water (bottom) deposited on the surface of melamine foam (white dice) and graphene-coated melamine foam (blackish dice). A dye (yellow for acetone and magenta for water) has been added to the droplets to render them more readily visible. Inset: magnified photograph of a water droplet on the surface of graphene-coated melamine foam. **(c,d)** FE-SEM images of the neat, non-coated melamine foam **(c)** and melamine foam coated with graphene **(d)**. **(e)** Digital photographs of: olive oil floating on water (left), a graphene-coated melamine foam adsorbing the oil phase (middle), and the final oil-free water after extraction of the sorbent (right). **(f)** Sorption capacity of graphene-coated melamine foam towards different organic solvents and oils. **(g)** Histogram for the re-usability of the graphene-coated foam for the sorption of oils.

The cathodically exfoliated material was also tested as an electrode for capacitive energy storage. Again in this case, the dried, as-expanded non-sonicated graphite material (0.3 M HTMABr) was preferred to the its solvent-sonicated counterpart for direct use as the electrode material, due to its easier processing and handling. The electrochemical charge storage experiments were carried out in a three-electrode configuration with aqueous 6M KOH as the electrolyte (see Experimental Section for details). Fig. 5a shows the cyclic voltammetry (CV) curves recorded for the as-expanded material at different potential scan rates. The voltammograms exhibited nearly rectangular shape with no redox peaks, indicating that charge storage in the electrode was dominated by the formation of an electric double layer, with no

significant contribution from Faradaic processes (i. e., pseudocapacitance). This is the expected behavior for carbon materials with low heteroatom content (including the present cathodic graphene), and thus low amounts of electroactive species (e.g., certain oxygen-containing functional groups) [60]. Fig. 5b shows typical galvanostatic charge/discharge curves recorded at different current densities for the as-expanded material. The curves displayed nearly symmetrical shapes and linear slopes, which is again consistent with electrochemical double-layer capacitive processes as the prevailing charge storage mechanism. As displayed in Fig. 5e (red squares), the gravimetric capacitance values calculated from the discharge curves for this material were ~25 F g^{-1} at 0.3 A g^{-1} and decreased down to ~5 F g^{-1} at a current density of 20 A g^{-1}. These figures were rather low in comparison with those reported for other graphene materials previously tested as electrodes for capacitive energy storage (see Table S2 in the Supplementary material for a comparative list). We interpret such a poor performance to be the result of significant re-stacking taking place in the material during its processing to form the electrodes. More specifically, re-stacking could readily arise from the drying and pressing of the cathodically expanded graphite. This re-stacking, together with the hydrophobic nature of the low-oxidized cathodic graphene layers, should prevent an effective wetting of interlayer spaces by the electrolyte, hence seriously limiting the capacitance of the electrode.

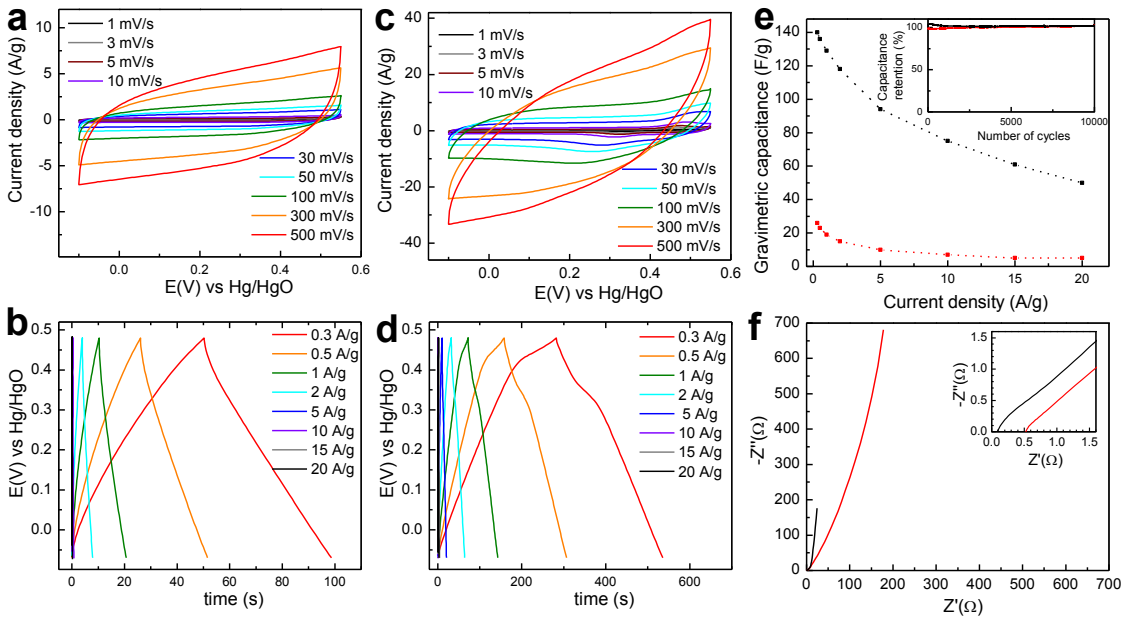

Figure 5. Electrode performance tests for catodically exfoliated graphite both alone and in combination with cobalt oxide nanosheets. Cyclic voltamograms recorded at potential scan rates between 1 and 500 mV/s for cathodic graphene alone **(a)** and cathodic graphene combined with cobalt oxide **(c)**. Galvanostatic charge/discharge curves recorded at current densities between 0.3 and 20 A/g for cathodic graphene alone **(b)** and cathodic graphene combined with cobalt oxide **(d)**. **(e)** Gravimetric capacitance values determined at different current densities from the discharge curves in b (red squares) and d (black squares). Inset to e: capacitance retention (in percentage) measured at a current density of 2 A/g for consecutive charge/discharge cycles (up to 10000) of the electrodes prepared from cathodic graphene alone (red trace), and cathodic graphene in combination with cobalt oxide (black trace). **(f)** Electrochemical impedance spectra of cathodic graphene alone (red trace) and cathodic graphene combined with cobalt oxide (black trace). Inset to f: detailed view of the high frequency region of the spectra.

To improve the capacitive performance of the cathodically expanded material, we combined it with a small amount of an electroactive material (cobalt oxide) in nanosheet morphology, which could provide a two-fold benefit: (1) to contribute pseudocapacitance to the hybrid electrode, and (2) to act as a spacer material within the expanded graphite, thus alleviating to some extent the issue of re-stacking during the electrode processing [60,63]. We synthesized cobalt oxide nanosheets following the general solvothermal method originally proposed by Sun et al for the preparation of stand-alone transition metal oxide nanosheets [36], but with the novelty that here the wet synthesis was performed in the presence of cathodically expanded graphite (see Experimental Section for details). The fact that the originally grey material acquired a slightly greenish tone after the process pointed to the successful generation of cobalt oxide [64]. Indeed, the amount of metal oxide present in the hybrid structure was determined to be ~5 wt% by elemental analysis. By comparison of the FE-SEM images of the surface of the as-expanded graphite before (Fig. 6a and c) and after (Fig. 6b and d) the solvothermal synthesis, we inferred that the small elongated features that uniformly decorated the surface of the latter correspond to cobalt oxide lamellae. Indeed, the nanosheets were seen to be attached sideways on to the expanded graphite plane, instead of lying flat on its surface. This morphology should be beneficial for the use of the material for capacitive energy storage, as it should increase the surface exposed to the electrolyte and improve accessibility of the ions. The presence of cobalt oxide on the expanded graphite was confirmed by XPS. Indeed, the recorded high resolution Co $2p_{3/2}$ core level spectrum (Fig. 6d) was that expected for cobalt in an oxidation state of +2 [65]. Indeed, the Co $2p_{3/2}$ band comprised a main peak located at a binding energy of ~781 eV, and a second, less intense satellite band at ~786 eV typical of cobalt (II) species.

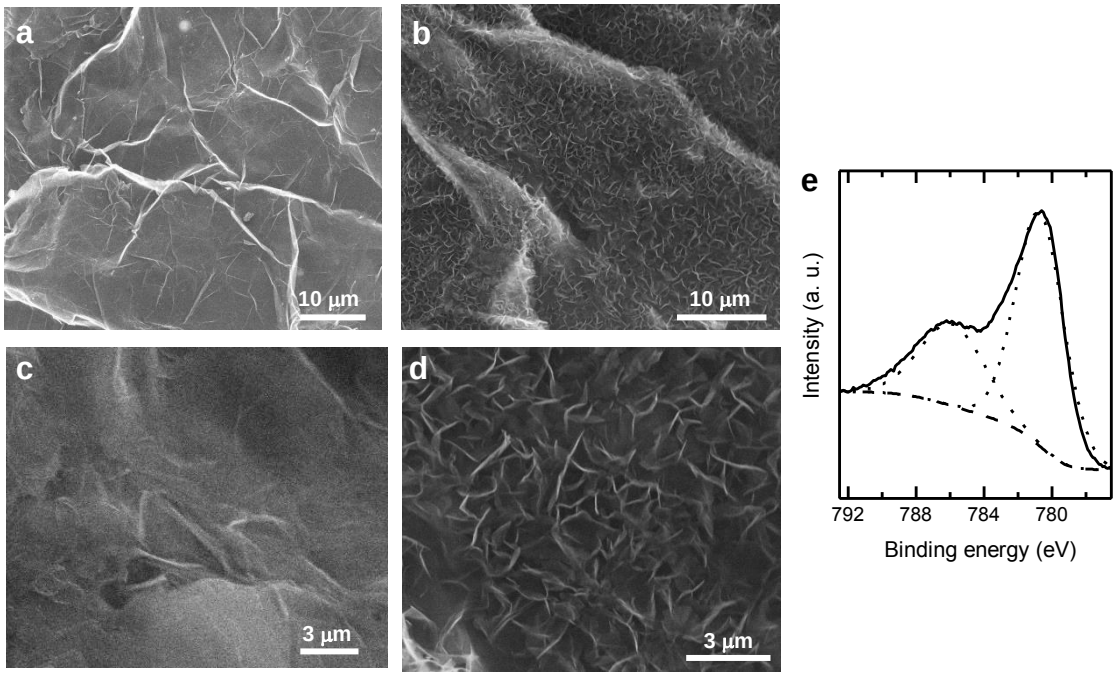

Figure 6. FE-SEM images of cathodically espanded graphite alone **(a,c)** and the same material coated with cobalt oxide nanosheets **(b,d)**. **(e)** High resolution Co $2p_{3/2}$ XPS spectrum of the expanded graphite-cobalt oxide hybrid. The background (dashed line), and the two components obtained upon peak-fitting of the spectrum (dotted lines) are also indicated.

The performance of the cathodicaly expanded graphite as an electrode was significantly improved by the small amount of cobalt oxide nanosheets, both in terms of delivered current (see Fig. 5c) and gravimetric capacitance values (Fig. 5e), the latter being 50–140 F g^{-1} for current densities ranging between 20 and 0.3 A g^{-1}. The occurrence of Faradaic redox reactions, in addition to purely capacitive processes, was confirmed by the appearance of oxidation and reduction humps visible in the CVs recorded at low potential scan rates (Fig. 5c) at potentials of ~0.45 V and ~0.3 V vs

Hg/HgO, respectively. The corresponding galvanostatic charge/discharge curves (Fig. 5d) were less symmetrical than those of its cobalt oxide-free counterpart (Fig. 5b), which was expected from the fact that some of the charge will be stored by ionic intercalation (pseudocapacitance) into the electrode and not just by the formation of an electrical double layer on its surface. This hybrid electrode was also stable, retaining its capacitance after 10,000 consecutive charge/discharge cycles at 2 A g^{-1} (black trace in the inset to Fig. 5e).

Information on ionic diffusion and electronic conductivity of the tested electrodes (with and without cobalt oxide), was obtained by electrochemical impedance spectroscopy. Fig. 5f shows Nyquist plots of the two electrodes. At high frequencies (inset to Fig. 5f) both materials behaved similarly, showing equivalent series resistance of ~0.1 Ω and ~0.5 Ω, for the electrodes with and without cobalt oxide, respectively. In the case of the cobalt oxide-containing materials, there was a short segment at 45° phase angle related to diffusion-controlled Faradaic reactions, followed by a nearly vertical line, indicative of an almost ideal capacitive behavior. However, the curve for the cobalt oxide-free material (red trace) exhibited a lower, similar phase angle largely independent of the frequency. This behavior has been previously observed for some porous carbon-based double-layer capacitors and is thought to have a non-diffusional origin related to the presence of a distributed resistor-capacitor network due to the porous nature of the electrode, where slit- and/or wedge-shaped pores lead to the kind of curve envelope observed here [66]. Indeed, such types of pore shape are the ones expected for graphenes obtained through electrochemical exfoliation (see Fig. 3).

4. Conclusions

We have demonstrated that high quality graphene nanosheets can be obtained in substantial yields (up to ~40–50 wt%) through cathodic exfoliation of graphite in water-based electrolytes. Two aspects were found to be critical for a successful and efficient aqueous cathodic exfoliation, namely, the type of starting graphite and the electrolyte. In the absence of oxidizing conditions during the electrolytic treatment such as those typically found in anodic exfoliation processes, the use of graphite materials having pre-expanded edges and interlayer voids (e.g., graphite foil) was seen to be essential for an effective intercalation of the material by aqueous cations. As for the electrolyte, quaternary ammonium-based cations of a certain intermediate size (e.g., tetrapropylammonium or hexyltrimethylammonium) exhibited an optimum ability to expand the graphite cathode and give graphene nanosheets in competitive yields. The exfoliated material could be colloidally dispersed in different media and was made up of few- to several-layer nanosheets with low defect content and limited oxidation. Melamine foam coated with cathodic graphene nanosheets was tested as a hydrophobic sorbent for the removal of oils and organic solvents from water, exhibiting good sorption capacities and a high re-usability. Likewise, combination of the cathodically exfoliated material with a small amount of vertically oriented cobalt oxide nanosheets afforded hybrids with good capacitive charge storage characteristics. Overall, we believe that the water-based route developed here should raise the prospects of cathodic exfoliation as a competitive approach in the efforts to industrialize the production of high quality graphene for use in different practical applications.

Supplementary material. Additional XPS characterization of the materials; additional FE-SEM characterization of graphite foil and HOPG; tables gathering a comparison of

the sorption capacity and gravimetric capacitance values of the materials prepared in this work with those previously reported for other graphene-based materials.

Acknowledgements

Funding by the Spanish Ministerio de Economía y Competitividad (MINECO) and the European Regional Development Fund (ERDF) through project MAT2015-69844-R is gratefully acknowledged. S.G-D. and J.M.M. are grateful to MINECO and the Spanish Ministerio de Educación, Cultura y Deporte (MECD), respectively, for their pre-doctoral contracts (FPU14/00792 and BES/2016 077830, respectively).

References

[1] F. Bonaccorso, L. Colombo, G. Yu, M. Stoller, V. Tozzini, A.C. Ferrari, R.S. Ruoff, V. Pellegrini, Production and Processing of Graphene and 2D Crystals, Science 347 (2015) 1246501.

[2] Y. Yang, C. Han, B. Jiang, J. Iocozzia, C. He, D. Shi, T. Jiang, Z. Lin, Graphene-Based Materials with Tailored Nanostructures for Energy Conversion and Storage, Mater. Sci. Eng. R 102 (2016) 1–72.

[3] M. Ye, Z. Zhang, Y. Zhao, L. Qu, Graphene Platforms for Smart Energy Generation and Storage, Joule 2 (2018) 245–268.

[4] K. C. Kemp, H. Seema, M. Saleh, N. H. Le, K. Mahesh, V. Chandra, K. S. Kim, Environmental applications using graphene composites: water remediation and gas adsorption, Nanoscale 5 (2013) 3149–3171.

[5] G. Ersan, O. G. Apul, F. Perreault, T. Karanfil, Adsorption of organic contaminants by graphene nanosheets: A review, Water Research 126 (2017) 385–398.

[6] V. Chabot, D. Higgins, A. Yu, X. Xiao, Zhongwei Chen, J. Zhang, A review of graphene and graphene oxide sponge: material synthesis and applications to energy and the environment, Energy Environ. Sci. 7 (2014) 1564–1596.

[7] P. C. Sherrell, C. Mattevi, Mesoscale Design of Multifunctional 3D Graphene Networks, Mater. Today 19 (2016) 428−436.

[8] C.T.J. Low, F.C. Walsh, M.H. Chakrabarti, M.A. Hashim, M.A. Hussain, Approaches to the Production of Graphene Flakes and their Potential Applications, Carbon 54 (2013) 1–21.

[9] H.J. Salavagione, Promising Alternative Routes for Graphene Production and Functionalization, J. Mater. Chem. A 2 (2014) 7138–7146.

[10] A.M. Abdelkader, A.J. Cooper, R.A.W. Dryfe, I.A. Kinloch, How to Get Between the Sheets: a Review of Recent Works on the Electrochemical Exfoliation of Graphene Materials from Bulk Graphite, Nanoscale 7 (2015) 6944–6956.

[11] S. Yang, M.R. Lohe, K. Müllen, X. Feng, New-Generation Graphene from Electrochemical Approaches: Production and Applications, Adv. Mater. 28 (2016) 6213–6221.

[12] J.I. Paredes, J.M. Munuera, Recent Advances and Energy-Related Applications of High Quality/Chemically Doped Graphenes Obtained by Electrochemical Exfoliation Methods, J. Mater. Chem. A 5 (2017) 7228–7242.

[13] D. Van Thanh, P. P. Oanh, D. T. Huong, P. H. Le, Ultrasonic-assisted cathodic electrochemical discharge for graphene synthesis, Ulttrason. Sonochem. 34 (2017) 978–983.

[14] J.M. Munuera, J.I. Paredes, M. Enterría, A. Pagán, S. Villar-Rodil, M.F.R. Pereira, J.I. Martins, J.L. Figueiredo, J.L. Cenis, A. Martínez-Alonso, J.M.D. Tascón, Electrochemical Exfoliation of Graphite in Aqueous Sodium Halide Electrolytes toward

Low Oxygen Content Graphene for Energy and Environmental Applications, ACS Appl. Mater. Interfaces 9 (2017) 24085–24099.

[15] C.-H. Chen, S.-W. Yang, M.-C. Chuang, W.-Y. Woon, C.-Y. Su, Towards the Continuous Production of High Crystallinity Graphene Via Electrochemical Exfoliation with Molecular In Situ Encapsulation, Nanoscale 7 (2015) 15362–15373.

[16] S. Yang, S. Brüller, Z.-S. Wu, Z. Liu, K. Parvez, R. Dong, F. Richard, P. Samorì, X. Feng, K. Müllen, Organic Radical-Assisted Electrochemical Exfoliation for the Scalable Production of High-Quality Graphene, J. Am. Chem. Soc. 137 (2015) 13927–13932.

[17] J.M. Munuera, J.I. Paredes, S. Villar-Rodil, M. Ayán-Varela, A. Martínez-Alonso, J.M.D. Tascón, Electrolytic Exfoliation of Graphite in Water with Multifunctional Electrolytes: En Route Towards High Quality, Oxide-Free Graphene Flakes, Nanoscale 8 (2016) 2982–2998.

[18] J. Wang, K.K. Manga, Q. Bao, K.P. Loh, High-Yield Synthesis of Few-Layer Graphene Flakes through Electrochemical Expansion of Graphite in Propylene Carbonate Electrolyte, J. Am. Chem. Soc. 133 (2011) 8888–8891.

[19] X. Cai, Y. Song, Z. Sun, D. Guo, X.-X. Liu, Rate Capability Improvement of Co−Ni Double Hydroxides Integrated in Cathodically Partially Exfoliated Graphite, J. Power Sources 365 (2017) 126–133.

[20] M. Zhou, J. Tang, Q. Cheng, G. Xu, P. Cui, L.-C. Qin, Few-layer Graphene Obtained by Electrochemical Exfoliation of Graphite Cathode, Chem. Phys. Lett. 572 (2013) 61–65.

[21] A.J. Cooper, N.R. Wilson, I.A. Kinloch, R.A.W. Dryfe, Single Stage Electrochemical Exfoliation Method for the Production of Few-Layer Graphene Via Intercalation of Tetraalkylammonium Cations, Carbon 66 (2014) 340–350.

[22] F. Ouhib, A. Aqil, J.-M. Thomassin, C. Malherbe, B. Gilbert, T. Svaldo-Lanero, A.-S. Duwez, F. Deschamps, N. Job, A. Vlad, S. Melinte, C. Jérôme, C. Detrembleur, A Facile and Fast Electrochemical Route to Produce Functional Few-Layer Graphene Sheets for Lithium Battery Anode Application, J. Mater. Chem. A 2 (2014) 15298–15302.

[23] A.T. Najafabadi, M.J. Leeuwner, D.P. Wilkinson, E.L. Gyenge, Electrochemically Produced Graphene for Microporous Layers in Fuel Cells, ChemSusChem 9 (2016) 1689–1697.

[24] A.T. Najafabadi, E. Gyenge, High-Yield Graphene Production by Electrochemical Exfoliation of Graphite: Novel Ionic liquid (IL]–Acetonitrile Electrolyte With Low IL Content, Carbon 71 (2014) 58–69.

[25] H. Lei, J. Tu, Z. Yu, S. Jiao, Exfoliation Mechanism of Graphite Cathode in Ionic Liquids, ACS Appl. Mater. Interfaces 9 (2017) 36702–36707.

[26] Yang, F. Lu, Z. Zhou, W. Song, Q. Chen, X. Ji, Electrochemically Cathodic Exfoliation of Graphene Sheets in Room Temperature Ionic Liquids N-Butyl, Methylpyrrolidinium Bis(trifluoromethylsulfonyl)imide and their Electrochemical Properties, Electrochim. Acta 113 (2013) 9–16.

[27] A.T. Najafabadi, E. Gyenge, Synergistic Production of Graphene Microsheets by Simultaneous Anodic and Cathodic Electro-Exfoliation of Graphitic Electrodes in Aprotic Ionic Liquids, Carbon 84 (2015) 449–459

[28] D. Vásquez-Sandoval, J. Pavez, C. Carlesi, A. Aracena. Large scale cathodic exfoliation of graphite using deep eutectic solvent and water mixture. Fuller. Nanotub. Car. N., 26 (2018) 123–129.

[29] G.M. Morales, P. Schifani, G. Ellis, C. Ballesteros, G. Martínez, C. Barbero, H.J. Salavagione, High-Quality Few Layer Graphene Produced by Electrochemical

Intercalation and Microwave-Assisted Expansion of Graphite, Carbon 49 (2011) 2809–2816.

[30] I. Jeon, B. Yoon, M. He, T.M. Swager, Hyperstage Graphite: Electrochemical Synthesis and Spontaneous Reactive Exfoliation, Adv. Mater. 30 (2018) 1704538.

[31] A. Ejigu, B. Miller, I.A. Kinloch, R.A.W. Dryfe, Optimisation of Electrolytic Solvents for Simultaneous Electrochemical Exfoliation and Functionalisation of Graphene with Metal Nanostructures, Carbon 128 (2018) 257–266.

[32] S. Yang, A.G. Ricciardulli, S. Liu, R. Dong, M.R. Lohe, A. Becker, M.A. Squillaci, P. Samorì, K. Müllen, X. Feng, Ultrafast Delamination of Graphite into High-Quality Graphene Using Alternating Currents, Angew. Chem. Int. Ed. 56 (2017) 6669–6675.

[33] H.-J. Butt, K. Graf, M. Kappl, Physics and Chemistry of Interfaces, Wiley-VCH, Weinheim, 2003, chapter 12.

[34] J. Oremusová, Micellization of Alkyl Trimethyl Ammonium Bromides in Aqueous Solutions–Part 1: Critical Micelle Concentration (CMC) and Ionization Degree, Tenside Surf. Det. 49 (2012) 231–240.

[35] M. Ayán-Varela, J.I. Paredes, L. Guardia, S. Villar-Rodil, J.M. Munuera, M. Díaz-González, C. Fernández-Sánchez, A. Martínez-Alonso, J.M.D. Tascón, Achieving Extremely Concentrated Aqueous Dispersions of Graphene Flakes and Catalytically Efficient Graphene-Metal Nanoparticle Hybrids with Flavin Mononucleotide as a High-Performance Stabilizer, ACS Appl. Mater. Interfaces 7 (2015) 10293–10307.

[36] Z. Sun, T. Liao, Y. Dou, S. M. Hwang, M.-S. Park, L. Jiang, J. H. Kim, S. X. Dou, Generalized Self-Assembly of Scalable Two-Dimensional Transition Metal Oxide Nanosheets. Nat. Commun. 5 (2014) 3813.

[37] K. Parvez, Z.-S. Wu, R. Li, X. Liu, R. Graf, X. Feng, K. Müllen, Exfoliation of Graphite into Graphene in Aqueous Solutions of Inorganic Salts, J. Am. Chem. Soc. 136 (2014) 6083–6091.

[38] J.M. Munuera, J.I. Paredes, S. Villar-Rodil, A. Castro-Muñiz, A. Martínez-Alonso, J.M.D. Tascón, High Quality, Low-Oxidized Graphene via Anodic Exfoliation with Table Salt as an Efficient Oxidation-Preventing Co-Electrolyte for Water/Oil Remediation and Capacitive Energy Storage Applications, Appl. Mater. Today 11 (2018) 246–254.

[39] M. Munuera, J.I. Paredes, S. Villar-Rodil, M. Ayán-Varela, A. Pagán, S.D. Aznar-Cervantes, J.L. Cenis, A. Martínez-Alonso, J.M.D. Tascón, High Quality, Low Oxygen Content and Biocompatible Graphene Nanosheets Obtained by Anodic Exfoliation of Different Graphite Types, Carbon 94 (2015) 729–739.

[40] M. Zhao, X.-Y. Guo, O. Ambacher, C.E. Nebel, R. Hoffmann, Electrochemical Generation of Hydrogenated Graphene Flakes, Carbon 83 (2015) 128–135.

[41] L. Wu, W. Li, P. Li, S. Liao, S. Qiu, M. Chen, Y. Guo, Q. Li, C. Zhu, L. Liu, Powder, Paper and Foam of Few-Layer Graphene Prepared in High Yield by Electrochemical Intercalation Exfoliation of Expanded Graphite, Small 10 (2014) 1421–1429.

[42] B.D. Ossonon, D. Bélanger, Synthesis and Characterization of Sulfophenyl-Functionalized Reduced Graphene Oxide Sheets, Carbon 111 (2017) 83–93.

[43] C. Boudon, M. Gross, F. Peter, Comparative Electrochemical Reduction of Ammonium and Potassium Chelates, J. Electroanal. Chem. 145 (1983), 181–187.

[44] O. Berkh, Y. Shacham-Diamand, E. Gileadi, Reduction of Ammonium Ion on Pt Electrodes, J. Electrochem. Soc. 155 (2008) F223–F229.

[45] J.A. Dean, Lange´s Handbook of Chemistry (15th edition), McGraw-Hill, New York, 1999, section 8.7.

[46] P. Vanýsek, Ionic Conductivity and Diffusion at Infinite Dilution, In: D.R. Lide (Ed.), CRC Handbook of Chemistry and Physics (83rd edition), CRC Press, Boca Raton, 2002.

[47] T. Wang, M.D.J. Quinn, S.M. Notley, Enhanced Electrical, Mechanical and Thermal Properties by Exfoliating Graphene Platelets of Larger Lateral Dimensions, Carbon 129 (2018) 191–198.

[48] D. Li, M.B. Müller, S. Gilje, R.B. Kaner, G.G. Wallace, Processable Aqueous Dispersions of Graphene Nanosheets, Nat. Nanotechnol. 3 (2008) 101–105.

[49] J.-W.T. Seo, A.A. Green, A.L. Antaris, M.C. Hersam, High-Concentration Aqueous Dispersions of Graphene using Nonionic, Biocompatible Block Copolymers, J. Phys. Chem. Lett. 2 (2011) 1004–1008.

[50] K. Erickson, R. Erni, Z. Lee, N. Alem, W. Gannett, A. Zettl, Determination of the Local Chemical Structure of Graphene Oxide and Reduced Graphene Oxide, Adv. Mater. 22 (2010) 4467–4472.

[51] M.A. Pimenta, G. Dresselhaus, M.S. Dresselhaus, L.G. Cançado, A. Jorio, R. Saito, Studying Disorder in Graphite-Based Systems by Raman Spectroscopy, Phys. Chem. Chem. Phys. 9 (2007) 1276–1291.

[52] L. Guardia, M. J. Fernández–Merino, J. I. Paredes, P. Solís–Fernández, S. Villar–Rodil, A. Martínez–Alonso, J. M. D. Tascón, High-Throughput Production of Pristine Graphene in an Aqueous Dispersion Assisted by Non-Ionic Surfactants, Carbon 49 (2011) 1653–1662.

[53] R. Paton, E. Varrla, C. Backes, R. J. Smith, U: Khan, A. O'Neill, C. Boland, M. Lotya, O. M. Istrate, P. King, T. Higgins, S. Barwich, P. May, P. Puczkarski, I. Ahmed,

M. Moebius, H. Pettersson, E. Long, J. Coelho, S. E. O'Brien, E. K. McGuire, B. Mendoza Sanchez, G. S. Duesberg, N. McEvoy, T. J. Pennycook, C. Downing, A. Crossley, V. Nicolosi, J. N. Coleman, Scalable Production of Large Quantities of Defect-Free Few-Layer Graphene by Shear Exfoliation in Liquids, Nat. Mater. 13 (2014) 624–630.

[54] U. Khan, A. O´Neill, M. Lotya, S. De, J. N. Coleman, High-Concentration Solvent Exfoliation of Graphene, Small 6 (2010) 864–871.

[55] L. Zhang, Z. Zhang, C. He, L. Dai, J. Liu, L. Wang, Rationally Designed Surfactants for Few-Layered Graphene Exfoliation: Ionic Groups Attached to Electron-Deficient π-Conjugated Unit through Alkyl Spacers, ACS Nano 8 (2014) 6663-6670.

[56] F. Zhou, H. Huang, C. Xiao, S. Zheng, X. Shi, J. Qin, Q. Fu, X. Bao, X. Feng, K. Müllen, Z.-S. Wu, Electrochemically Scalable Production of Fluorine-Modified Graphene for Flexible and High-Energy Ionogel-Based Microsupercapacitor, J. Am. Chem. Soc. 140 (2018) 8198–8205.

[57] Y.L. Zhong, T.M. Swager, Enhanced Electrochemical Expansion of Graphite for in Situ Electrochemical Functionalization, J. Am. Chem. Soc. 134 (2012), 17896–17899.

[58] H. Huang, Y. Xia, X. Tao, J. Du, J. Fang, Y. Gan, W. Zhang, Highly Efficient Electrolytic Exfoliation of Graphite into Graphene Sheets Based on Li Ions Intercalation–Expansion–Microexplosion Mechanism, J. Mater. Chem. 22 (2012) 10452–10456.

[59] F. Li, M. Xue, X. Zhang, L. Chen, G.P. Knowles, D.R. MacFarlane, J. Zhang, Advanced Composite 2D Energy Materials by Simultaneous Anodic and Cathodic Exfoliation, Adv. Energy Mater. 8 (2018) 1702794.

[60] R. Raccichini, A. Varzi, S. Passerini, B. Scrosati, The role of graphene for electrochemical energy storage, The Role of Graphene for Electrochemical Energy Storage, Nat. Mater. 14 (2015) 271–279.

[61] P. C. Sherrell, C. Mattevi, Mesoscale Design of Multifunctional 3D Graphene Networks, Mater. Today 19 (2016) 428−436.

[62] D. D. Nguyen, N.-H. Tai, S.-B. Lee, W.-S. Kuo, Superhydrophobic and Superoleophilic Properties of Graphene-Based Sponges Fabricated Using a Facile Dip Coating Method. Energy Environ. Sci. 5 (2012) 7908–7912.

[63] B. Chen, Q. Ma, C. Tan, T.-T. Lim, L. Huang, H. Zhang, Carbon-Based Sorbents with Three-Dimensional Architectures for Water Remediation, Small 11 (2015) 3319–3336.

[64] Greenwood, N. N.; Earnshaw, A.. Chemistry of the Elements. Pergamon Press. Oxford, 1984; Chapter 26: Cobalt, Rhodium and Iridium.

[65] S. J. Cochran, F. P. Larkins, Surface Reduction of some Transition-Metal Oxides. an X-Ray Photoelectron Spectroscopic Study of Iron, cobalt, Nickel and Zinc Oxides. J. Chem. Soc., Faraday Trans. 81 (1985) 2179–2190.

[66] B. E. Conway, Electrochemical Supercapacitors. Scientific Fundamentals and Technological Applications. Kluwer Academic/Plenum Publishers, New York, 1999; pp. 401, 509.